Molecular mode-coupling theory applied to a liquid of diatomic molecules

A. Winkler,[1] A. Latz,[1,*] R. Schilling, and C. Theis[2]
[1]*Institut für Physik, Johannes Gutenberg-Universität, Staudinger Weg 7, D-55099 Mainz, Germany*
[2]*Fakultät für Physik, Albert-Ludwigs-Universität, Hermann-Herder-Straße 3, D-79104 Freiburg, Germany*
(Received 17 July 2000)

We study the molecular mode-coupling theory for a liquid of diatomic molecules. The equations for the critical tensorial nonergodicity parameters $\mathbf{F}^m_{ll'}(q)$ and the critical amplitudes of the β relaxation $\mathbf{H}^m_{ll'}(q)$ are solved up to a cutoff $l_{co}=2$ without any further approximations. Here l,m are indices of spherical harmonics. Contrary to previous studies, where additional approximations were applied, we find in agreement with simulations that all molecular degrees of freedom vitrify at a single temperature T_c. The theoretical results for the nonergodicity parameters and the critical amplitudes are compared with those from simulations. The qualitative agreement is good for all molecular degrees of freedom. To study the influence of the cutoff on the nonergodicity parameter, we also calculate the nonergodicity parameters for an upper cutoff $l_{co}=4$. In addition, we also propose a method for the calculation of the critical nonergodicity parameter from the liquid side of transition.

PACS number(s): 61.25.Em, 64.70.Pf, 61.43.Fs, 61.20.Ja

I. INTRODUCTION

The mode-coupling theory (MCT) of the glass transition is by now an important tool to understand experiments in and simulations of supercooled liquids [1]. For a long time, most of the theoretical investigations concentrated on simple monatomic or binary liquids. All universal and even system-specific predictions of these investigations could be tested on a *quantitative* level in a system of hard colloids [2,3], which is an excellent realization of a hard-sphere system, and in computer simulations for a binary Lennard-Jones system [4,5]. Details of theory and tests for simple glass formers can be found in review articles [6–12] and articles cited therein.

Although the theory was originally formulated only for these simple systems, most of the experimental and simulation support came from research on much more complex systems [e.g., tri-α-naphtylbenzene [13], Orthoterphenyl (OTP) [14–17], $0.4Ca(NO_3)_20.6KNO_3$ (CKN) [18–21], Glycerol [22–24], Salol [25–27], toluene [28], and water [29,30]]. Also most of the experimental methods used did *not* measure density correlation functions or their susceptibilities, for which the original theory was formulated. Even neutron-scattering experiments in systems consisting of molecules whose components have different cross sections for neutrons [17,23,28] do not measure the density correlation function exclusively, but rather a mixture of more complicated correlation functions involving molecular degrees of freedom [31] (see also [32] for a single linear molecule). Dielectric loss measurements [21,24] measure directly the correlation function of a tensor of rank 1. Depolarized light scattering [14,19,25,33], Kerr effect experiments [34,35], nuclear magnetic resonance [36–38], and electron-spin resonance [39] (and references therein) measure correlation function of a tensor of rank 2. The mentioned tensorial quantities are all related to orientational degrees of freedom (ODOF), whereas the original theory [40] only considered translational degrees of freedom (TDOF), i.e., the center-of-mass motion. But of course, when comparing experimental results on complex systems with predictions of the MCT for simple liquids, it was always reasonable to argue that there are in every experiment couplings to the center-of-mass motion. For example, reorientation of dipoles measured in dielectric loss measurements can be induced by the center-of-mass motion via a translation-rotation coupling. Also the reorientation of the polarizability tensor in light scattering measurements is related to a physical rotation of the molecules and will therefore be coupled to the center-of-mass motion of the molecules as well. A slowing down of this motion due to very slow structural relaxations can consequently also indirectly be measured in the mentioned experiments. In addition, it is perfectly justified to perform tests of the *universal* predictions of MCT in complicated molecular and polymeric systems [41] for β-scaling laws and properties of the α relaxation, such as the time temperature superposition principle and wave-vector-dependent stretching exponents, since the underlying universal features of the bifurcation scenario should also remain valid for molecular systems.

But beyond the universal aspects, MCT aims to be a microscopic theory of structural relaxation. This goal is to a large extent achieved for simple liquids. There it was possible to obtain quantitative agreement between experiment and theory for the full dynamic range of structural relaxation (i.e., β and α region) [2,3,5]. Recently, also a theory for anomalous high-frequency oscillations (Bose peak phenomenon) was formulated within MCT [42]. The molecular mode-coupling theory (MMCT), which has been under study for a few years now, intends to extend this line of research to experimentally relevant molecular systems. There are three different mode-coupling theories for the description of different aspects of molecular degrees of freedom. In [32,43], the motion of a single linear molecule in a liquid of spherical atoms is studied. In [44], a site-site description is formulated, which is perfectly adapted to study neutron-scattering experiments of molecular systems. In this approach, the atomic structure of the molecules is considered. Finally, the MMCT

*Author to whom correspondence should be addressed.

[45] that we are using in this work [46] is devised to investigate the dynamics of a liquid of linear molecules. For this purpose, a self-consistent mode-coupling theory for the dynamic correlation functions of tensorial densities $\rho_{lm}(\vec{q},t)$ was developed. These densities are the generalized Fourier components of the microscopic density $\rho(\vec{x},\Omega)$ in an expansion in spherical harmonics with respect to the orientation $\Omega=(\theta,\varphi)$ of the molecules and plane waves with respect to $\vec{x}$. An extension to arbitrary molecules is given in [47]. A theory for arbitrary molecules was also formulated in [48]. First results for the tensorial nonergodicity parameters (NEP) and critical amplitudes were obtained for dipolar hard spheres [46] and [49], respectively. A study of the phase diagram for glass transitions of a liquid of hard ellipsoids was performed in Ref. [50]. Several aspects of the theory for general molecules were tested against simulation for water in Refs. [51,52] and treating water as a linear molecule in Ref. [47].

As in the MCT for simple liquids, the static structure factors $S^m_{ll'}(q)$ in the q frame, i.e., the coordinate system in which the z axis is along the wave vector, completely determine the long-time dynamics and thus the NEP and critical amplitudes. Note that the structure factors (static and dynamic) are diagonal in m in the q frame [46]. The static structure factors have to be known to solve the equations of MMCT. They are either obtained by analytical theories as, e.g., in Refs. [53–55] for ellipsoids or they have to be taken from simulations. In this work, we present a detailed comparison of MMCT calculations of the NEP and critical amplitudes with the results of simulation for a liquid of diatomic molecules. A detailed description of the system and the simulation can be found in [56,57]. There, tests of the universal properties of MCT are also presented. For our comparison between simulation and theory, the static structure factors are taken from the simulation. In a preliminary study, only the diagonal static correlators $S^m_{ll}(q)$ were used as input and also the dynamical correlators $S^m_{ll}(q,t)$ and thus the NEP were assumed to be diagonal [58]. This severe approximation has led to unphysical results such as the existence of two different transition temperatures for ODOF and TDOF. In our study, we use diagonal *and* nondiagonal elements of the static structure factor as input to calculate *all* components of the NEP and, in addition, of the critical amplitudes. For the calculation of the NEP, we also extend the necessary upper cutoff l_{co} for the index l to $l_{\mathrm{co}}=4$.

The paper is organized as follows. In Sec. II, we review the main equations and concepts for the calculation of the critical NEP (Sec. II A) and the critical amplitudes (Sec. II B). In Sec. III, we discuss the influence of different approximation schemes on the theoretically obtained critical temperatures (Sec. III A) and their relation to simulation results. Then we present the comparison of theoretical critical NEP (Sec. III B) and critical amplitudes (Sec. III C) with simulations. Conclusions are presented in Sec. IV and an Appendix describes how the critical NEP can be obtained from the liquid side close the the ideal glass transition.

II. MOLECULAR MODE-COUPLING THEORY

A. Nonergodicity parameter

The derivation of the equation of MMCT for the dynamics of linear molecules and general molecules can be found in [46] and [47], respectively. We only repeat the basic definitions and equations and refer the reader for details to the literature. For the present work, in which we want to calculate the critical NEP and the critical amplitudes of diatomic molecules, we only need the equations for linear molecules in the limit of time to infinity. The basic quantities are the correlation functions of tensorial densities $\rho_{lm}(\vec{q},t)$ and tensorial current densities $j^{\alpha}_{lm}(\vec{q},t)$,

$$\rho_{lm}(\vec{q},t)=\sqrt{4\pi}i^l\sum_{n=1}^{N}e^{i\vec{q}\cdot\vec{x}_n(t)}Y_{lm}(\vec{\Omega}_n(t)). \tag{1}$$

$$\vec{j}^{\alpha}_{lm}(\vec{q},t)=\sqrt{4\pi}i^l\sum_{n=1}^{N}\vec{v}^{\alpha}_n e^{i\vec{q}\cdot\vec{x}_n(t)}Y_{lm}(\vec{\Omega}_n(t)). \tag{2}$$

The $Y_{lm}(\vec{\Omega}_n(t))$ are the standard spherical harmonics and we follow in our notation the textbook by Gray and Gubbins [59]. $\vec{v}^{\alpha}_n$ is either the center-of-mass velocity $\vec{v}_n(t)$ of the nth molecule or its angular velocity $\vec{\omega}_n(t)$ depending on the index α:

$$\vec{v}^{\alpha}_n(t):=\begin{cases}\vec{v}_n(t), & \alpha=T\\ \vec{\omega}_n(t), & \alpha=R,\end{cases} \tag{3}$$

where T and R stand for the translational and rotational part, respectively. For the calculation of the NEP, we need in principle all spatial components of the currents but here we use as in [46] only the projection on directions defined by the wave vector $\vec{q}$ and the angular momentum operator $\vec{L}$. Taking into account also transversal currents will lead only to a small correction in the NEP [60]. We therefore define the *longitudinal* currents $j^{\alpha}_{lm}(\vec{q},t)$,

$$j^{\alpha}_{lm}(\vec{q},t)=\frac{1}{q^{\alpha}_l}(\hat{q}^{\alpha}\vec{j}^{\alpha})_{lm}(\vec{q}), \quad \alpha\in\{T,R\} \tag{4}$$

with

$$q^{\alpha}_l(q):=\begin{cases}q, & \alpha=T\\ \sqrt{l(l+1)}, & \alpha=R\end{cases} \tag{5}$$

and the definition

$$\hat{q}^{\alpha}:=\begin{cases}\vec{q}, & \alpha=T\\ \vec{L}, & \alpha=R.\end{cases} \tag{6}$$

The quantities we are going to calculate are NEP $F^m_{ll'}(q)$ in the q frame, i.e., in a coordinate system in which the z axis is given by the direction of the wave vector $\vec{q}=(0,0,q)$. In this coordinate system, all correlation functions $\langle\rho^*_{lm}(\vec{q},t)\rho_{l'm'}(\vec{q},0)\rangle=\delta_{mm'}S^m_{l,l'}(q,t)$ are diagonal in m. They are real and depend on $|m|$ only. The same holds for all other tensorial quantities that we will use in the q frame. The NEP are given by

$$F^m_{ll'}(q)=\lim_{t\to\infty}S^m_{ll'}(q,t). \tag{7}$$

As input for the mode-coupling equations, we need the static structure factors $S^m_{ll'}(q)$. They are directly taken from the simulation of Kämmerer *et al.* [57]. The system, investigated there, is a one-component system of rigid diatomic molecules. Each molecule is composed of two different Lennard-Jones particles, denoted by *A* and *B*. They have the same mass and are separated by a distance $d=0.5\sigma_{AA}$, where σ_{AA} is the Lennard Jones parameter of atom *A*. The interaction between two molecules is given by the sum of the interaction between the four particles, which is given by the Lennard-Jones potential $V_{\alpha,\beta}(r)=4\varepsilon_{\alpha,\beta}[(\sigma_{\alpha,\beta}/r)^{12}-(\sigma_{\alpha,\beta}/r)^{-6}]$, where $\alpha,\beta\in\{A,B\}$. The exact choice of the simulation parameters can be found in [56]. The off-diagonal elements of the static structure factors were not yet published and had to be determined from the raw data.

The equation for the matrix $\mathbf{F}(q)\equiv F^m_{ll'}(q)$ of NEP can then be written [46] as

$$\mathbf{F}(q)=[\mathbf{1}+\boldsymbol{\mathcal{K}}(q)\mathbf{S}^{-1}(q)]^{-1}\mathbf{S}(q). \tag{8}$$

The matrix $\boldsymbol{\mathcal{K}}$ is related to the Laplace transform of the dynamic current correlation function and can be expressed as the inverse of a memory matrix $\boldsymbol{\mathcal{F}}^m(q)\equiv\mathcal{F}^m_{ll'}(q)$ at $t=\infty$,

$$\mathcal{K}^m_{ll'}(\vec{q})=\sum_{\alpha\alpha'} q^\alpha_l(q)[\boldsymbol{\mathcal{F}}^m(q)^{-1}]^{\alpha\alpha'}_{ll'} q^{\alpha'}_{l'}(q). \tag{9}$$

The mode-coupling approximations yield

$$\mathcal{F}^{m\alpha\alpha'}_{ll'}(q)\approx\frac{1}{2N}\left(\frac{\rho_0}{4\pi}\right)^2{\sum_{\vec{q}_1\vec{q}_2}}'\sum_{m_1m_2}\sum_{l_1l_2}\sum_{l'_1l'_2}V^{\alpha\alpha'}_{ll'l_1l'_1l_2l'_2}\times(q,q_1,q_2;m,m_1,m_2)F^{m_1}_{l_1l'_1}(q_1)F^{m_2}_{l_2l'_2}(q_2), \tag{10}$$

with

$$V^{\alpha\alpha'}_{ll'l_1l'_1l_2l'_2}(q,q_1,q_2;m,m_1,m_2):=v^\alpha_{ll_1l_2}(q,q_1,q_2;m,m_1,m_2)v^{\alpha'}_{l'l'_1l'_2}(q,q_1,q_2;m,m_1,m_2)^*, \tag{11}$$

$$v^\alpha_{ll_1l_2}(q,q_1,q_2;m,m_1,m_2):=\sum_{l_3}u^\alpha_{ll_3l_2}(q,q_1,q_2;m,m_1,m_2)\times c^{m_1}_{l_3l_1}(q_1)+(-1)^m(1\leftrightarrow2), \tag{12}$$

and

$$u^\alpha_{ll_1l_2}(q,q_1,q_2;m,m_1,m_2):=i^{l_1+l_2-l}\left[\frac{(2l_1+1)(2l_2+1)}{(2l+1)}\right]^{1/2}\tfrac{1}{2}[1+(-1)^{l_1+l_2+l}]\times\sum_{m'_1m'_2}(-1)^{m'_2}d^{l_1}_{m'_1m_1}(\Theta_{q_1})d^{l_2}_{m'_2m_2}(\Theta_{q_2})\times C(l_1l_2l;m'_1m'_2m)\times\begin{cases}q_1\cos\Theta_{q_1}C(l_1l_2l;000); & \alpha=T\\ \sqrt{l_1(l_1+1)}\,C(l_1l_2l;101); & \alpha=R.\end{cases} \tag{13}$$

Here the functions $C(l_1l_2l;m_1,m_2,m)$ are the Clebsch-Gordan coefficients and $d^l_{m'm}(\Theta)$ are related to Wigner's rotation matrices (we follow the notation of Gray and Gubbins). For given Euler angles $\Omega=(\Phi,\Theta,\chi)$, they are defined as [59]

$$D^l_{mm'}(\Omega)=e^{-im\Phi}d^l_{mm'}(\Theta)e^{-im'\chi}. \tag{14}$$

Θ_{q_i} is the angle between $\vec{q}$ and $\vec{q}_i$. The prime at the first summation in Eq. (10) restricts $\vec{q}_1,\vec{q}_2$ such that $\vec{q}_1+\vec{q}_2=\vec{q}$. Equations (8)–(10) form a closed set of infinitely many coupled nonlinear equations for the NEP. To obtain a solvable theory, we have to restrict l to be smaller than an upper cutoff, $l\leqslant l_{\mathrm{co}}$. The resulting equations can in principle be solved by a fixed-point iteration algorithm. Physical control parameters such as the temperature and the density only enter via the static structure factor. At a critical temperature or density, the solution of this equation bifurcates from all functions $F^m_{ll'}(q)$ being zero to nonzero. In the simulations of Kämmerer *et al.* [56,57], the temperature was used as a control parameter. Close to the transition temperature T_c, the stability matrix of the iteration (see below) will have the largest eigenvalue E_0 approaching $E_0=1$ from below. Consequently, the convergence of the iteration is very slowly getting close to T_c. The time for one iteration depends very sensitively on the upper cutoff l_{co}. For $l_{\mathrm{co}}=2$, one iteration took 10 min on a MIPS R10000; for $l_{\mathrm{co}}=4$ this time increased to 6 h. We therefore concentrated on $l_{\mathrm{co}}=2$ to determine the transition point with a high accuracy and used the calculation for $l_{\mathrm{co}}=4$ mostly as a check for the sensitivity of our results against changing the cutoff.

To overcome some of the restrictions connected to the critical slowing down of the convergence close to T_c, we determined the critical NEP, i.e., the NEP at T_c, with two alternative methods. For the standard fixed-point iteration we started at a temperature low enough to be in the glass state. Then the temperature is increased very slowly. At every temperature, the equations for the NEP are solved by the iteration

$$\mathbf{F}^{(n+1)}(q)=\boldsymbol{\mathcal{G}}(\mathbf{F}^n,\boldsymbol{\epsilon}), \tag{15}$$

where $\boldsymbol{\mathcal{G}}(\mathbf{F}^{(n)})$ is the right-hand side of Eq. (8) and $\boldsymbol{\epsilon}=(T_c-T)/T_c$. This iteration converges exponentially fast towards its solution as long as the temperature is not the critical temperature. The convergence rate is determined by the largest eigenvalue E_0 of the stability tensor $\mathcal{C}_{\lambda\lambda'}=\partial\mathcal{G}_\lambda/\partial F_{\lambda'}$ [61].

The index λ is an abbreviation for wave vectors q and rotational indices l,l',m. The exponential convergence rate is then $\ln E_0$. Close to and below T_c, the eigenvalue E_0 can be written as $E_0=1-A\sqrt{\epsilon}$, with A being a positive constant. Therefore, the convergence rate is $A\sqrt{\epsilon}$ and the number of iterations to obtain convergence diverges inversely proportional to $\sqrt{\epsilon}$ close to T_c. With this number of iterations, the deviations of our NEP from the true critical NEP are proportional to $\sqrt{\epsilon}$, since the NEP exhibit the well-known square root singularity (cf. [6]).

If the temperature is increased above T_c, i.e., $\epsilon<0$, there is no nonzero solution for the iteration Eq. (15). Nevertheless, for $0<-\epsilon\ll 1$ the iteration is nearly stationary for a large number of iterations of the order $|\epsilon|^{-1/2}$ (see the Appendix). The approximate critical NEP is determined as the stationary point $\hat{\mathbf{F}}(\epsilon)$, whose change along the eigenvector with eigenvalue 1 of the *critical* stability matrix is minimal during iteration. But contrary to the NEP determined from the fixed-point iteration for $T<T_c$, the stationary NEP differ only in order $|\epsilon|$ instead of in order $\sqrt{\epsilon}$ from the true critical NEP. Consequently, this property allows us in the following to cross-check the very accurate results for $l_{\mathrm{co}}=2$ obtained from the fixed-point iteration and also to obtain the critical NEP for $l_{\mathrm{co}}=4$.

B. Critical amplitudes

A central prediction of the mode-coupling theory of the glass transition in simple liquids is the existence of the β-scaling regime [62,63,6]. For the problem of a single dumbbell in an isotropic hard-sphere system [32], it was demonstrated that the β-scaling law can be detected in every quantity that couples to the density. For a liquid of anisotropic molecules, it is not very well defined which degree of freedom is driving the glass transition. The equations of MMCT couple all degrees of freedom and there are situations where the transition is not caused by the TDOF but rather the ODOF [50]. But even in these systems, the factorization theorem is generically valid for all correlators. This can be proven using the standard techniques [6]. Therefore, every dynamic structure factor $S^m_{ll'}(q,t;T)$ for $-1\ll\epsilon\ll 1$ in the β region can be written as

$$S^m_{ll'}(q,t;T)=F^m_{ll'}(q)+H^m_{ll'}(q)G(t/t_0;\sigma). \tag{16}$$

The function $G(t/t_0)$ is the same for all l,l',m,q. t_0 is an overall microscopic scale. $H^m_{ll'}(q)$ are the critical amplitudes determining the intensity of the asymptotic β-scaling law for a certain combination of l, l', m, and q. Also, the correction to the asymptotics, which determine, besides the temperature, the range of validity of the law Eq. (16), depends on these amplitudes (cf. Ref. [64] for simple liquids). Differences in the observability of the critical correlators between depolarized light-scattering experiments and dielectric loss measurements can be explained by differences in the amplitudes $H^m_{ll'}(q)$ involving $l=2$ and $l=1$, respectively (see Ref. [43] for a single molecule). To determine the amplitudes numerically to a high precision, it is necessary to be very close to the transition point to make sure that all correction terms of order ϵ are small compared to the leading term of order $\sqrt{\epsilon}$. Due to the difficulties described above, we could only determine the critical amplitudes for upper cutoff $l_{\mathrm{co}}=2$.

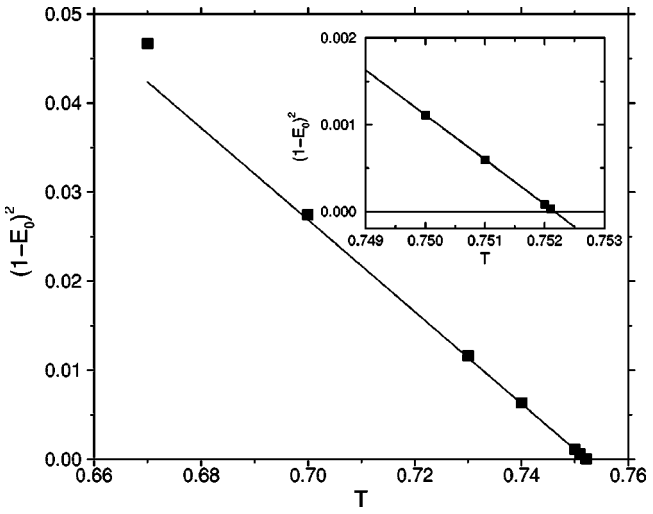

FIG. 1. The square deviation of the largest eigenvalue of the stability matrix (see text) from its critical value $E_0(T_c)=1$ as a function of temperature. The full line is a linear fit $(1-E_0)^2\propto(T_c-T)^2$ to the data with $T_c=0.752\,15$. The inset shows a magnification for the same quantity very close to T_c.

III. RESULTS

A. The critical temperatures

For $l_{\mathrm{co}}=2$ and in the full diagonalization approximation [58], in which the static structure factors $\mathbf{S}(q)$, the glass form factors $\mathbf{F}(q)$, and the memory matrix $\mathcal{F}(q)$ are assumed to be diagonal with respect to l, the glass transition temperature for the TDOF predicted by MMCT is below the transition temperature of the MD simulations $T_c^{\mathrm{MD}}=0.477$. Note that these temperatures are given in Lennard-Jones units (cf. [56]). In all other known examples, the MCT overestimates the tendency for vitrification. As an additional artifact of the full diagonalization, the ODOF vitrify at a lower temperature than the TDOF. Since the top-down symmetry of the dumbbells is broken, the full equations of MMCT (8)–(10) generically do not allow for such a scenario. As soon as we take $\mathbf{S}(q)$ nondiagonal, all degrees of freedom undergo a glass transition at the same temperature above the MD result. To study the influence of different diagonalization approximations in a bit more detail, we investigated several cases, with the main condition of $\mathbf{S}(q)$ being nondiagonal: (i) $\mathbf{F}(q)$ and $\mathcal{F}(q)$ diagonal (dd); (ii) $\mathbf{F}(q)$ diagonal and $\mathcal{F}(q)$ nondiagonal (dnd); (iii) $\mathbf{F}(q)$ and $\mathcal{F}(q)$ nondiagonal (ndnd).

Let us discuss $l_{\mathrm{co}}=2$ first. For this case, T_c has been determined very accurately from the asymptotic behavior $[1-E_0(T)]^2\propto\epsilon$ (see Sec. II B) for the largest eigenvalue $E_0(T)$. Figure 1 demonstrates this law for case (iii). The highest transition temperature is obtained for case (i). Here the transition temperature is roughly three times as large as the MD result, $T_c^{dd}=1.4$. In case (ii), it only slightly decreases to $T_c^{\mathrm{dnd}}=1.38$. If everything is taken nondiagonal [case (iii)], the transition temperature is $T_c=0.7521$. Al-

though still twice as large as the MD result, the discrepancy of this result from T_c^{MD} is comparable to other known cases and consistent with the usual 20% accuracy of the critical *density* [5]. The equations are too complex to get a deeper theoretical understanding of this seemingly erratic jumping of the transition temperature, dependent on the approximation we are using. Particularly, the fact that the vertices [Eq. (12)] are not positive anymore makes an analytical prediction impossible. But it is at least possible to rationalize the behavior using a combination of physical and mathematical arguments. First of all, it is quite clear that the full diagonalization where all matrices are assumed to be diagonal is too crude to describe the coupling of TDOF and ODOF for the system of diatomic molecules. The TDOF and ODOF are only coupled via the diagonal memory function $\mathcal{F}_{ll'}^{m\alpha\alpha'}(q)$. The coupling of the equations for different l is considerably reduced compared to the case where $\mathbf{S}(q)$ is taken to be nondiagonal. For example, in the $\mathcal{F}_{00}^{mTT}(q)$ component of the memory matrix, only terms of the form (symbolically) $\Sigma_{l',m'} V_{l'}^{m'} (F_{l'l'}^{m'})^2$ appear in the full diagonalization approximation, since the Clebsch-Gordan coefficients $C(0l'l'',0,m',m'')$, which enter into the vertices [cf. Eqs. (10)–(13)], are nonzero for $l'=l''$ only. Similarly, the memory functional $\mathcal{F}_{11}^{m\alpha\alpha'}(q)$ only contains couplings of the form $F_{00}^0 F_{11}^m$ and $F_{22}^m F_{11}^m$. For $\mathcal{F}_{22}^{m\alpha\alpha'}(q)$, the Clebsch-Gordan coefficients in the vertex allow ''self''-couplings $(F_{11}^m)^2$, $(F_{22}^m)^2$, and couplings to $l=0$ in the form $F_{00}^0 F_{22}^m$, but no ''self''-couplings $(F_{00}^0)^2$. Due to the absence of $(F_{00}^0)^2$ in $\mathcal{F}_{22}^{m\alpha\alpha'}(q)$, a freezing of the center-of-mass motion, i.e., $l=l'=0$, does not imply a freezing for quadrupolar dynamics $l=l'=2$. If the vertex for the coupling of the NEP with $l=2$ and $l=0$ in F_{11}^m and F_{22}^m is not large enough, exactly this structure of the memory matrix allows generically a separate transition of the $l=0$ and the $l\neq 0$ components of the diagonalized dynamic structure factor as observed in [58]. But we have to stress that the approximation is not inadequate *per se*. In the case of water [51], the full diagonalization approximation leads to a rather satisfactory agreement with simulations, without the artifact of separate transitions and too low transition temperatures. The pronounced angular dependence of interaction between water molecules, which is reflected in the fact that the static structure factors for $l=2$, $m=0,1,2$, and $l=0$ are of the same order, yields large enough vertices to produce a single transition temperature of the TDOF and ODOF. In the present case, the structure factor S_{00}^0 is clearly more dominant than S_{22}^m (see Fig. 2). This is different from water, where all m for $l=l'=2$ are important. This leads to the *a posteriori* conclusion that in general the full diagonalization can only be used (if at all) for systems with ''very strong'' static translation rotation coupling. This statement, unfortunately, cannot be further quantified.

If we now take the nondiagonality of $\mathbf{S}(q)$ seriously but leave all other matrices diagonal [case (i)], *additional* coupling between TDOF and ODOF appears, which may lead to an effectively stronger coupling. Although the equations for the different l components of the NEP still couple only via the diagonal memory functions $\mathcal{F}_{ll}^{m\alpha\alpha'}(q)$, the diagonalized memory matrix contains now *static* couplings between *all* NEP. For example, $\mathcal{F}_{11}^{m\alpha\alpha'}(q)$ contains additional couplings between the TDOF correlator F_{00}^0 and the correlators involving $l=2$ and, even more important, ''self-coupling'' terms $(F_{00}^0)^2$ due to the nonvanishing structure factors S_{10}^0 and $S_{12}^m(q)$, respectively. This of course does not explain, but at least makes plausible the dramatic increase of the transition temperature. Any slowing down of, say, the TDOF is immediately transferred to all other degrees of freedom and causes a further slowing down of the TDOF due to the feedback via the memory function. This enhances the tendency towards vitrification and also is responsible for the existence of a single transition temperature.

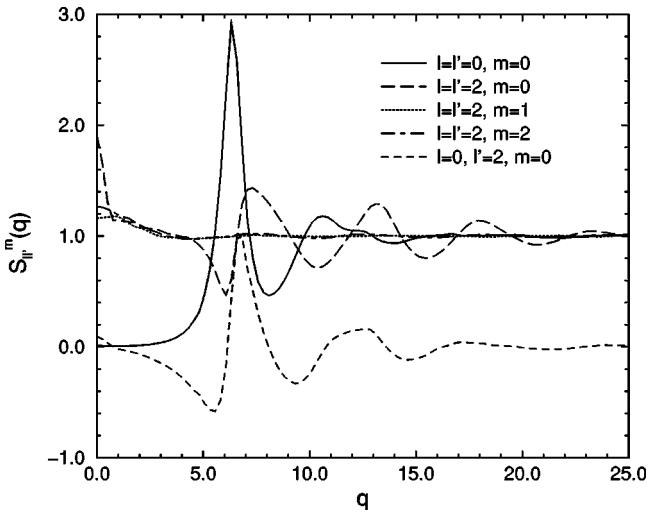

FIG. 2. A selection of structure factors $S_{ll'}^m(q)$ of a liquid of diatomic molecules in the q frame at temperature $T=0.7521$ and pressure $p=1$ in Lennard-Jones units. The full curve is the structure factor $S_{00}^0(q)$, the long dashed curve is $S_{22}^0(q)$, the dotted curve is $S_{22}^1(q)$, the dashed-dotted curve is $S_{22}^2(q)$, and the short dashed curve is $S_{02}^0(q)$.

The reason for the decrease of the transition temperature, when we give up the diagonalization approximations for $\mathcal{F}(q)$ and $\mathbf{F}(q)$ [case (iii)], is not obvious. We only note that the transition temperature is decreasing from case (i) ($T_c=1.4$) over (ii) ($T_c=1.38$) to (iii) ($T_c=0.752$), i.e., the more off-diagonal elements of the matrix $\boldsymbol{\mathcal{F}}$ are taken into account. $\boldsymbol{\mathcal{F}}$ is the $t\to\infty$ limit of the memory matrix, i.e., the random force correlation function. Therefore, it seems that the more components of the random forces are coupled, the lower is the transition temperature. This implies that the more the random forces can mutually influence each other, the more difficult it is to form a glass. Although we cannot prove this statement on mathematical grounds, it describes a feasible physical phenomenon.

To test the sensitivity of our results to changes in the cutoff, we also solved the MMCT for upper cutoff $l_{\mathrm{co}}=4$. The larger cutoff value for l reduces the transition temperature further towards the simulation result. For $l_{\mathrm{co}}=4$, an upper and a lower bound for T_c have been determined. The lower bound is the highest temperature for which the NEP are still nonzero after 88 iterations. The upper bound is the temperature for which the NEP are converging to zero after about 24 iterations. Since the time per iteration increases

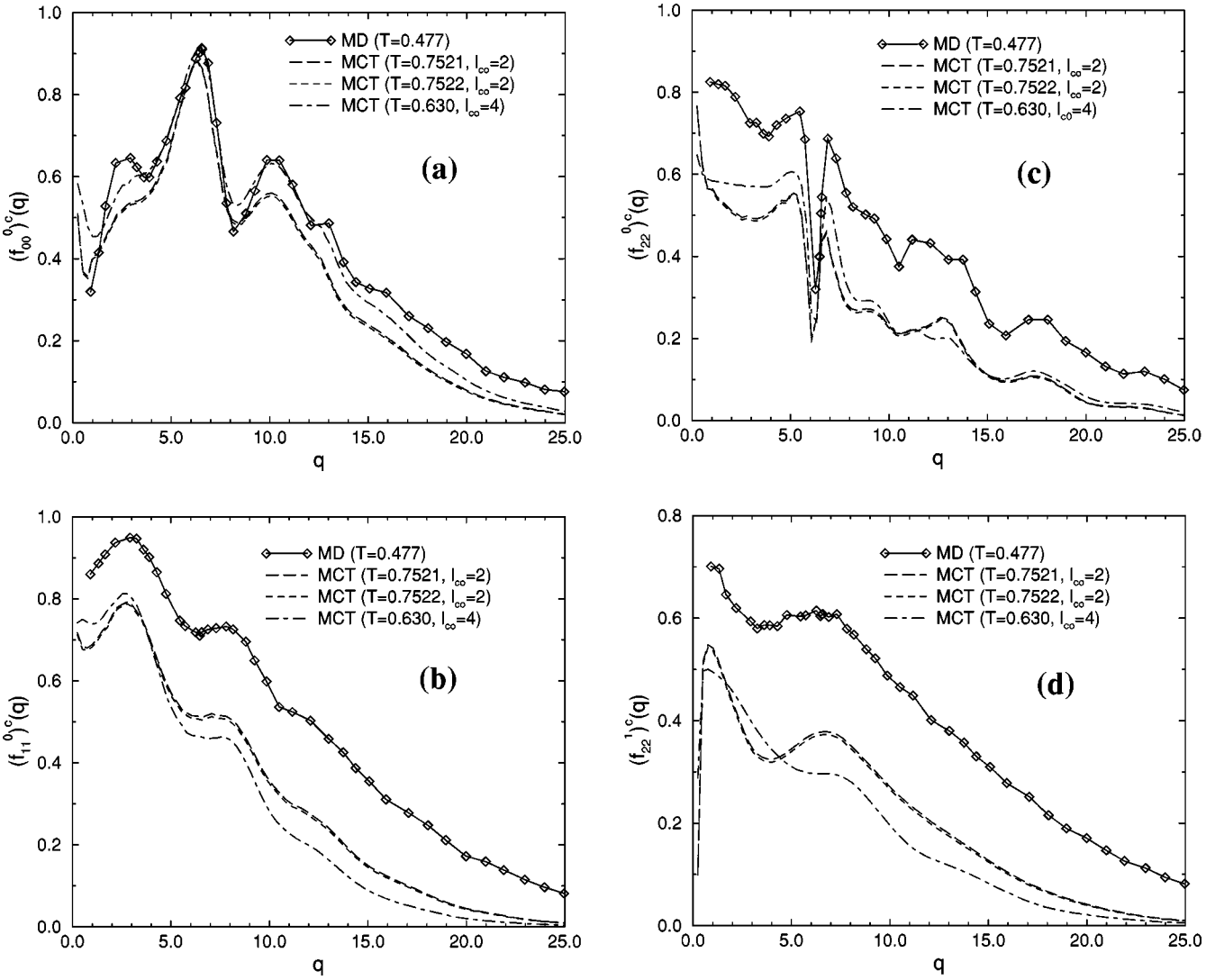

FIG. 3. Normalized diagonal elements $f^m_{ll}(q)$ of the nonergodicity parameter matrix. As normalization, the corresponding diagonal elements of the static structure factor are used. Shown are the elements for $(l,m)=(0,0)$ (a), $(l,m)=(1,0)$ (b), $(l,m)=(2,0)$ (c), and $(l,m)=(2,1)$ (d). The full line is the result of the simulation at $T=0.477$ obtained by fitting a von Schweidler law plus corrections of order $(t/\tau_\alpha)^{2b}$ to the simulation data. The estimated critical temperature is $T_c=0.475$. The long dashed line is the result of the fixed-point iteration for upper cutoff $l_{\rm co}=2$ at $T=0.7521$ slightly below the theoretical $T_c=0.752\,15$. The short dashed curve is the result of the quasistationary criterion for upper cutoff $l_{\rm co}=2$ at $T=0.7522$ slightly above the theoretical T_c. The dashed-dotted curve is the result of the quasistationary criterion for upper cutoff $l_{\rm co}=4$ at $T=0.630$ (above the theoretical T_c) for $l_{\rm co}=4$.

dramatically upon increasing the upper cutoff, the transition temperature could only be determined within 5%, $T_c=0.61$. It is encouraging that the real transition is approached upon increasing the cutoff, but our arguments presented above show that this is not necessarily the case. Which of the competing mechanisms influencing the transition temperature is dominant cannot be predicted on general grounds.

B. The nonergodicity parameters

In the following, we concentrate on the results for the normalized NEP $f^m_{ll'}(q)=F^m_{ll'}(q)/\sqrt{S^m_{ll}(q)S^m_{l'l'}(q)}$ without any diagonalization approximation. Figure 3 shows the normalized diagonal terms of the matrix of NEP $f^m_{ll}(q)$ for $(l,m)=(0,0),(1,0),(2,0),(2,1)$. Not shown are the results for $(l,m)=(1,1),(2,2)$, since they do not exhibit very much structure. The corresponding simulation result is taken from [57]. It was obtained by fitting a von Schweidler law plus corrections $S^m_{ll'}(q,t)=F^m_{ll'}(q)-H^m_{ll'}(q)(t/\tau_\alpha)^b+(H^{(2)})^m_{ll'}(q)(t/\tau_\alpha)^{2b}$ to the simulation results for the time-dependent density correlation function $S^m_{ll'}(q,t)$, where τ_α is the α-relaxation scale. There are three different theoretical curves. The two curves at temperatures $T_c=0.7522,0.7521$ are obtained with the fixed-point method (on the glass side of the transition) and the quasistability criterion (on the liquid side), respectively, as described above for upper cutoff $l_{\rm co}=2$. Their good agreement demonstrates the high accuracy of the solution. The third theoretical curve shows the result for upper cutoff $l_{\rm co}=4$ using the more accurate quasistability criterion. Compared to the results in [58], a clear improvement of the agreement with simulations can be observed. Especially, the q dependence of the functions is very well

reproduced. Even a feature like the prepeak in $f^0_{00}(q)$ at $q \sim 2.5$ is reproduced as a shoulder in the corresponding theoretical result. This peak is not present in the static structure factors. Since $S^0_{11}(q)$ has a peak at about $q \sim 2.5$, it could appear due to a dynamic coupling of the ODOF, especially the one involving $l=1$ and the TDOF. Note also that the mentioned peak exactly corresponds to the first peak in $f^0_{11}(q)$. There is a tendency that the agreement is best around the wave vector, where the structure factor $S_{00}(q)$ has its first peak and is getting worse for large wave vectors. This might be interpreted as an indication for the glass transition being driven also for the investigated system of diatomic molecules by the TDOF. From investigations of other systems [46,49,50], we know that different scenarios are possible.

Similar to increasing q, the agreement between simulation and theory gets worse with increasing l. This is expected due to two different reasons. First, higher l correspond to a higher angular resolution and are therefore probably much more affected by the mode-coupling approximation. Second, higher l are of course much more sensitive to the cutoff l_{co} than lower l. The curves for larger cutoff increase the quality of the comparison with the MD results. But it is important to note that in our case no general rule can be given as to how much the quality of the results for lower values of l can be improved by increasing the upper cutoff, as this was done in [32]. In the case of a single dumbbell in a liquid of hard spheres, the glass transition temperature is completely determined by the hard-sphere liquid and does not change by increasing the cutoff l_{co}. As explained above, in our case T_c can depend very sensitively on l_{co}. But this influences directly the amplitude of the NEP via the trivial effect of the temperature on the static structure factors. We already compensate as much as possible for this mechanism by presenting only the *normalized* NEP. But as in the case of hard spheres, there is still the effect that also the normalized NEP are proportional to the static structure factor. This is a very nontrivial phenomenon, since the existence of negative vertices in the mode-coupling functional $\boldsymbol{\mathcal{F}}(q)$ could in principle lead to a violation of this correlation. But as can be inferred from Fig. 3, the NEP $f^0_{00}(q), f^0_{22}(q)$ for $l_{\mathrm{co}}=4$ are systematically larger than that for $l_{\mathrm{co}}=2$ in a large region around the first peak of the structure factor $S^0_{00}(q)$, without big differences in the functional form. This effect, especially for $F^0_{00}(q)$ where the mentioned trend is valid for all wave vectors, can be mainly understood as a consequence of the transition temperature being smaller for $l_{\mathrm{co}}=4$ than for $l_{\mathrm{co}}=2$, which causes the first peak of $S^0_{00}(q)$ to increase. Additional evidence for this reasoning is presented in Fig. 4. In this figure, we show the results for $l_{\mathrm{co}}=4$ at temperature $T=0.60$, obtained with the fixed-point method, and $T=0.63$, obtained with the quasistability criterion. The lower temperature is still in the glass (the required accuracy, i.e., the maximum difference between consecutive iterates, which is smaller than 10^{-6}, is reached after 88 iterations). At the higher temperature, the accuracy is first increasing as expected (see the Appendix). But after 24 iterations, it begins slowly to decrease and after 42 iterations the iterates start to converge quickly towards the solution $\mathbf{F}(q)=0$. The results for the lower temperature agree, except for $l=0$, much better with the simulation than the one for the higher temperature. But since the deviations to the true critical NEP at roughly the same number of iterations are of order $|T-T_c|$ for the higher temperature compared to order $\sqrt{|T-T_c|}$ for the lower one, we have to conclude that the results for the higher temperature are closer to the critical NEP of the theory. The better agreement with simulations of the NEP at $T=0.600$ is a trivial consequence of the fact that positive NEP increase with decreasing temperature. Due to this influence of the value of T_c on the amplitude of the normalized critical NEP, we cannot in general conclude that increasing the cutoff l_{co} leads to a better agreement with the simulation. It might even happen that the agreement with simulations gets worse instead of better, if increasing the cutoff would lead to a larger transition temperature. This is possible due to the existence of negative vertices in the mode-coupling functional $\boldsymbol{\mathcal{F}}$.

The observed trends allow the reasonable hypothesis that the temperature effect could be the main source for the deviations between simulation and theory. In general, the main structural features in the normalized nonergodicity parameter are very well represented, but they are systematically too small for nearly all wave vectors, exactly as expected, if the theoretical transition temperature is too large.

Figure 5 demonstrates that the theory also gives good results for the off-diagonal NEP. We found that S^0_{02} and F^0_{02} are the only important off-diagonal components of the static structure factor matrix $\mathbf{S}(q)$ and NEP matrix $\mathbf{F}(q)$, respectively. In Fig. 5, we therefore show the normalized NEP f^0_{02}. The quality of the result is even better than for the diagonal components of the NEP.

C. Critical amplitudes

The critical amplitudes are determined only up to an overall scale factor. That is, our theoretical results cannot be directly compared to the simulation results. But once we have chosen a scale factor for, e.g., the amplitude h^0_{00}, all other amplitudes should be multiplied with the same scale factor to compare with the simulations. In Fig. 6(a), we have chosen a scale factor of 200 to obtain the best agreement with the normalized critical amplitude $h^0_{00}(q)=H^0_{00}(q)/S^0_{00}(q)$. The features of this component are the same as in simple glass forming systems [65–67,4]. There is a minimum at the position of the first peak of $S^0_{00}(q)$. Simulations and theory compare quite well for $2 \leqslant q \leqslant 7$ and show deviations at other wave vectors. With the chosen scale factors, the other diagonal elements of the critical amplitude matrix show strong deviations from the simulation results. Especially, $h^0_{11}(q)$ [see Fig. 6(b)] does not even disagree in amplitude nor in the form, except for the minimum at $q \sim 3$. This is not unexpected, since the simulations have shown strong differences between the form of the dynamic correlators involving odd and even l [57]. Due to the weak top-down anisotropy of our diatomic molecules, the dynamic of the correlators involving odd l is only weakly coupled to the dynamics of the even components [43]. 180° jumps are still possible on a much faster time scale than the translational motion [57]. Consequently, there are strong corrections to the asymptotic results for the correlator $S^0_{11}(q,t)$ and the amplitude $h^0_{11}(q)$ is not very well defined.

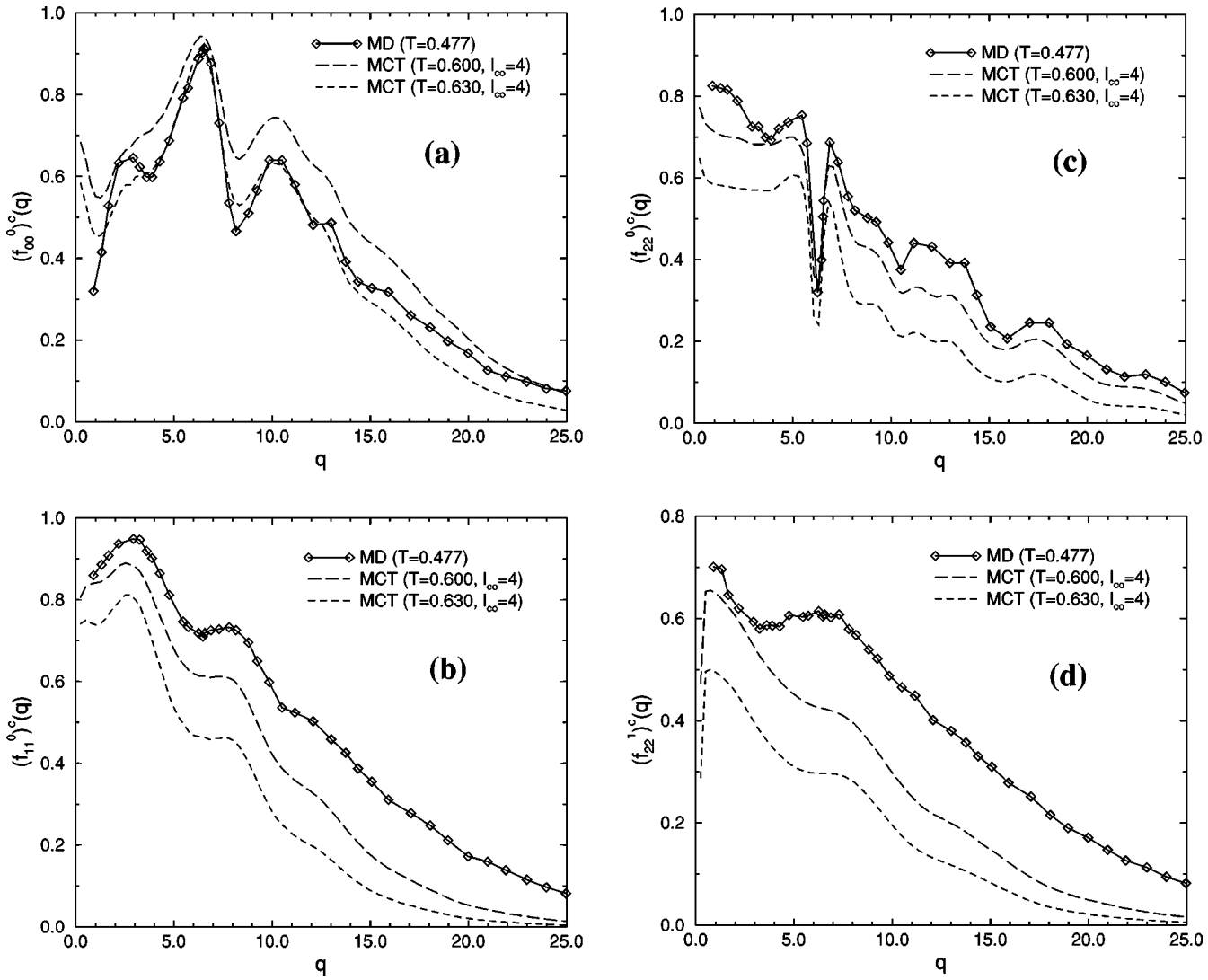

FIG. 4. Normalized diagonal elements $f_{ll}^{m}(q)$ of the nonergodicity parameter matrix for $l_{\mathrm{co}}=4$ obtained with the fixed-point method and stationary criterion, respectively, in comparison with simulation. As normalization, the corresponding diagonal elements of the static structure factor are used. Shown are the elements for $(l,m)=(0,0)$ (a), $(l,m)=(1,0)$ (b), $(l,m)=(2,0)$ (c), and $(l,m)=(2,1)$ (d). The full line is the result of the simulation at $T=0.477$. The long dashed line is the result of the fixed-point iteration for upper cutoff $l_{\mathrm{co}}=4$ at $T=0.600$. The short dashed curve is the result of the quasistationary criterion for upper cutoff $l_{\mathrm{co}}=4$ at $T=0.630$.

The deviations between simulation and theory in h_{22}^{0} [see Fig. 6(c)] are more serious, since $S_{22}^{0}(q,t)$ exhibits a well-defined β region. We can improve the agreement between simulation and theory by choosing a free scale factor for the simulation curves. The result is shown in Fig. 6(d) to demonstrate, in contrast to h_{11}^{0}, that essential structural features in h_{22}^{0} are indeed reproduced by the theory. As argued above, the dynamic correlators and therefore also the critical amplitudes involving $l=2$ are much more affected by the cutoff $l_{\mathrm{co}}=2$ than the one with lower l. This might be the reason for the rather large discrepancy found for h_{22}^{0}. To determine the critical amplitudes, it is necessary to be very close to the critical point. Restriction in computer time did not allow us to determine T_c for $l_{\mathrm{co}}=4$ with high enough accuracy to get reliable results for the critical amplitudes.

The critical amplitudes with $m>0$ do not exhibit very much structure. In Fig. 7, we show for completeness the result for $h_{22}^{1}(q)$, which could in principle be measured in light scattering experiments. Again we choose an overall amplitude prefactor as a free fit parameter, but the agreement is still not very good. Much better is the agreement (similar to the NEP) for h_{02}^{0} (see Fig. 8), although we still had to choose the amplitude scale of the simulation as a free fit parameter.

IV. CONCLUSIONS

We have performed a quantitative test of MMCT for a liquid of diatomic molecules. The static structure factors from simulations were used as input for the MMCT to calculate the critical temperature T_c, the matrix of critical NEP $F_{ll'}^{m}(q)$, and the matrix of critical β-scaling amplitudes $H_{ll'}^{m}(q)$. Several approximation schemes were used to test the sensitivity of the results against changing the degree of diagonalization of the $F_{ll'}^{m}(q)$ in l and l' and the dependence on the upper cutoff l_{co}. As maximum cutoff, $l_{\mathrm{co}}=4$ was used. Since the computational effort increases strongly with l_{co}, we used a more accurate method to determine the critical NEP from the liquid side of the transition.

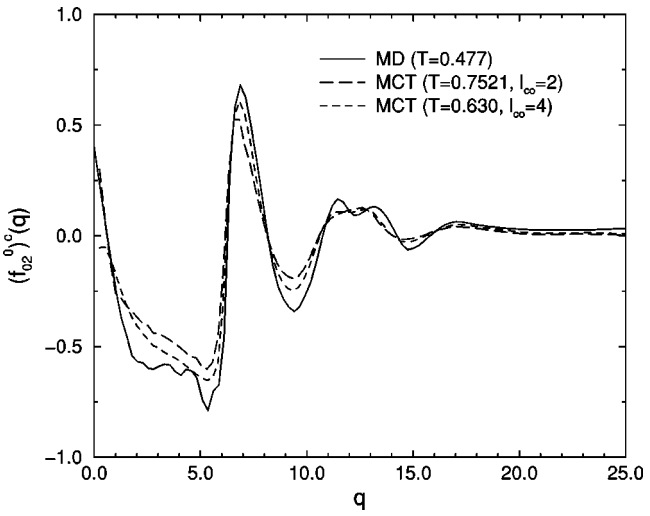

FIG. 5. Normalized off-diagonal elements $f^0_{02}(q)$ of the nonergodicity parameter matrix. As normalization, $\sqrt{S^0_{00}S^0_{22}}$ was chosen. The full line is the result of the simulation at $T=0.477$. The long dashed line is the result of the fixed-point iteration for upper cutoff $l_{co}=2$ at $T=0.7521$. The short dashed curve is the result of the quasistationary criterion for upper cutoff $l_{co}=4$ at $T=0.630$.

As expected, by giving up any diagonalization approximation for $S^m_{ll'}(q)$, $F^m_{ll'}(q)$, and the memory functional $\mathcal{F}^{m\alpha\alpha'}_{ll'}(q)$, all degrees of freedom vitrify at a single temperature. In fact, to obtain a unique transition temperature, it is sufficient to keep only the static structure factor $S^m_{ll'}(q)$ nondiagonal in l and l'. The strongest effect of successively applying diagonalization approximations for the NEP $F^m_{ll'}(q)$ and the memory functional $\mathcal{F}^{m\alpha\alpha'}_{ll'}(q)$ is the change of the transition temperatures T_c. Also using different cutoffs l_{co} changes the transition temperature.

Contrary to T_c, the overall form of NEP is much less sensitive to the different approximation schemes. The agreement with simulation is qualitatively quite good for cutoff $l_{co}=2$ as well as for $l_{co}=4$. In some cases, especially for the $l=0,l'=0$ component and the off-diagonal $l=0,l'=2$ component of the NEP, the agreement is even quantitative for wave vectors around the first peak of the structure factor $S^0_{00}(q)$. The comparison of the NEP with simulations for the correlator with $(l=0,l'=0)$ is clearly improved using the cutoff $l_{co}=4$ instead of $l_{co}=2$. Other correlators are better represented for $l_{co}=2$. We therefore cannot conclude that in general a further increase of the cutoff will lead necessarily to still better agreement with simulations.

Also the wave-vector dependence of the normalized critical β-scaling amplitudes agrees quite well with the one obtained from simulations. Contrary to the prediction of MMCT, no common amplitude scale for the critical amplitudes with different l and l' could be found. At present, it is not clear whether this failure is real or due to the fitting procedure used in [57] to obtain the beta relaxation amplitudes. Also the restriction to cutoff $l_{co}=2$ for the determination of the critical amplitudes could cause the found discrepancies, since also correlators with $l>2$ will contribute to the critical amplitudes at $l=2$. By neglecting them, an error in the amplitude scale is possible.

In summarizing our study, we may say that the MMCT offers an overall consistent description of the glass transition in molecular liquid of diatomic molecules, at least concerning the critical NEP and the critical amplitudes.

ACKNOWLEDGMENTS

It is a pleasure to thank W. Götze for a critical reading of the manuscript. We are grateful to the Sonderforschungsbereich 262 for financial support.

APPENDIX: DETERMINATION OF THE NEP USING QUASISTABILITY

If the temperature is chosen above the critical temperature, the only stable fixed point of the iteration (15) is $\mathbf{F}=0$. But there is still the possibility of determining the critical NEP with even higher accuracy than with the converging iteration for $T<T_c$. To implement the method, we have to initialize the iteration with $F^{(0)}_\mu$, which is close to F^c_μ, where μ is a superindex for q, l, l', and m. This can be achieved by first using the fixed-point iteration

$$F^{(n+1)}_\mu = \mathcal{G}_\mu(\{F^{(n)}_{\mu'}\},\epsilon) \tag{A1}$$

below T_c and increasing the temperatures in small steps until the liquid regime is reached. The critical temperature will eventually be missed by a small value $0<-\epsilon\ll 1$ and the iteration converges after a *long* transient quickly to zero. Since the iteration at a given temperature is always initialized with the final result of the previous temperature, the above assumption is fulfilled. The long transient is caused by the marginal stability of the critical point. The iteration will be dominated for a long time by the critical direction of the iteration, which is given by the eigenvector e^c, which belongs to the eigenvalue $E_0=1$ of the *critical* stability matrix $(C^c_{\mu\mu'})=(\partial\mathcal{G}_\mu/\partial F_{\mu'})^c$ [61]. The NEP $\hat{F}_\mu(\epsilon)$ at which the iteration is almost stationary is given by minimizing the distance of the projection of $\Delta C_\mu=\mathcal{G}_\mu(\{F_{\mu'},\epsilon\})-F_\mu$ on the critical direction $\hat{e}^c$, where for technical reasons the *left* critical eigenvector $\hat{e}^c$ was chosen. This condition can be written as

$$\frac{\partial\sum_\mu \hat{e}^c_\mu \Delta C_\mu}{\partial F_{\mu'}} = \sum_\mu \hat{e}^c_\mu C_{\mu\mu'}(\{\hat{F}_{\mu''}\},\epsilon) - \hat{e}^c_{\mu'} = 0. \tag{A2}$$

Equation (A2) determines the quasistationary point $\hat{F}_\mu(\epsilon)$, such that matrix $C_{\mu\mu'}(\{\hat{F}_{\mu''},\epsilon\})$ has an eigenvalue $\hat{E}_0(\epsilon)=1$ for $\epsilon<0$. $\epsilon<0$ indicates that the temperature is $T=T_c(1-\epsilon)>T_c$. This stationary point $\hat{F}_\mu$ differs from F^c_μ in order ϵ. This can be proven by using an argument analogous to deriving the β-scaling equation [6]. Defining $\hat{\delta}_\mu$ by $\hat{F}_\mu=F^c_\mu+\hat{\delta}_\mu$ and using the property that $C_{\mu\mu'}(\{\hat{F}_{\mu''}\},\epsilon)$ is a smooth differentiable function of ϵ, Eq. (A2) can be written, in leading order in $\hat{\delta}_\mu$ and ϵ, as

$$0=\sum_\mu \hat{e}^c_\mu\left(\sum_{\mu''} C_{\mu\mu'\mu''}(\mathbf{F}^c,0)\,\hat{\delta}_{\mu''} + \left.\frac{\partial C_{\mu\mu'}(\mathbf{F}^c,\epsilon)}{\partial\epsilon}\right|_{\epsilon=0}\epsilon\right). \tag{A3}$$

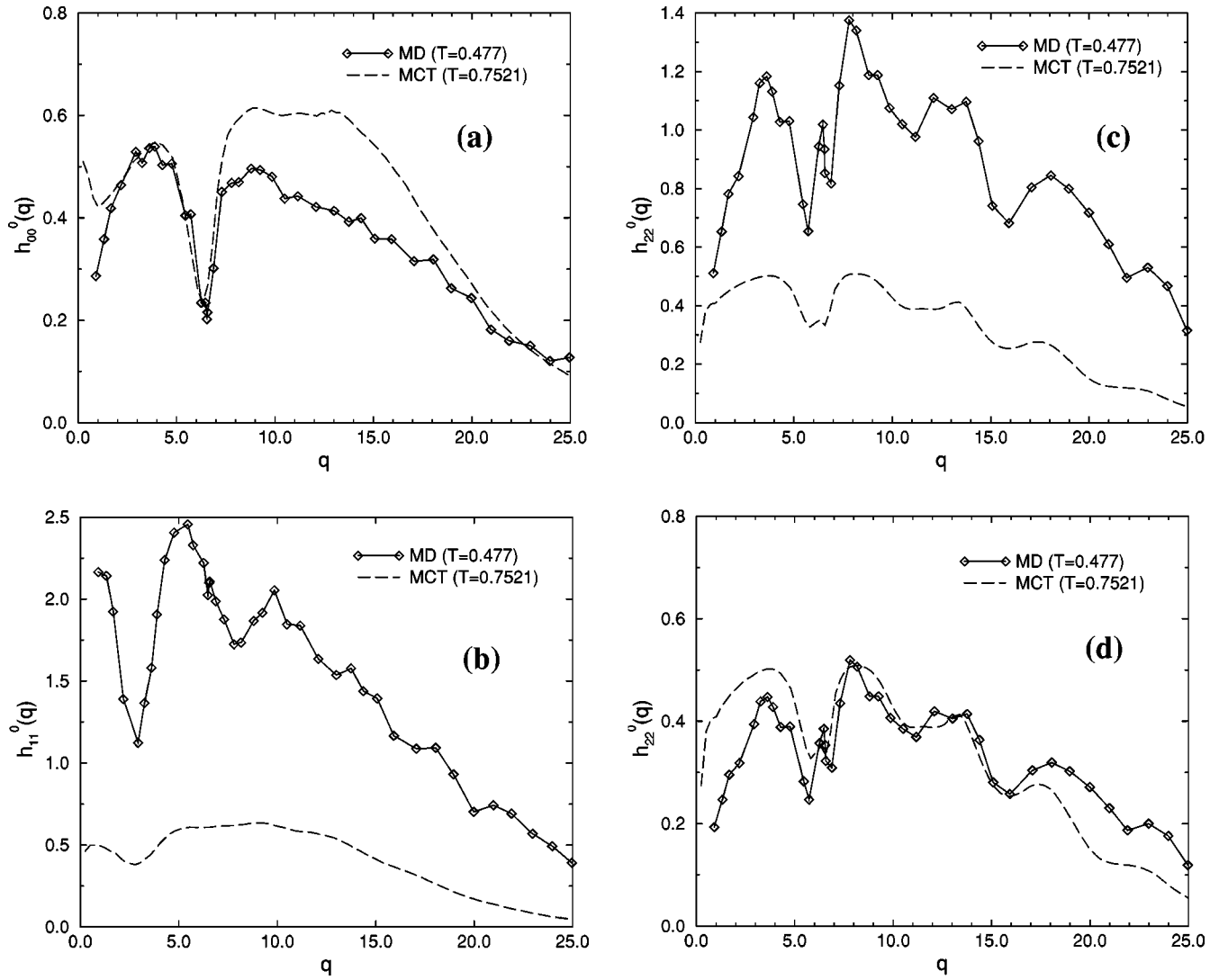

FIG. 6. Normalized diagonal elements $h_{ll}^{m}(q)$ of the matrix of critical amplitudes. As normalization, the corresponding diagonal elements of the static structure factor are used. The result of the simulation at $T=0.477$ is obtained by fitting a von Schweidler law plus corrections of order $(t/\tau_\alpha)^{2b}$ to the simulation data. The fits to the simulations (full lines) are multiplied with a factor 200 (see text for details) to obtain the best agreement with the theoretical result for $h_{00}^{0}(q)$. Shown are the theoretical results for $T=0.7521$, upper cutoff $l_{\mathrm{co}}=2$. (a)–(c) show the results for $(l,m)=(0,0)$, $(1,0)$, and $(2,0)$, respectively. The dashed curve is always the result of the theory. (d) shows again the same theoretical result as in (c), but the free scale factor of the critical amplitude of the simulation is chosen to optimize the agreement with theory (see text for details).

Here we have in addition used that $\hat{e}_\mu^c$ is the left eigenvector of the stability matrix at the critical point with eigenvalue $E_0=1$. The tensor $C_{\mu\mu'\mu''}$ is the partial derivative of the stability matrix with respect to $F_{\mu''}$. Equation (A3) immediately shows that $\hat{\delta}_\mu$ is (at least) of order ϵ. Note that the argument crucially depends on the well-known phenomenon that static quantities such as the structure factors, which determine completely the stability matrix $(C_{\mu\mu'}(\{F_{\mu''}\},\epsilon)$, are varying smoothly across the glass transition.

We now want to estimate the number of iterations required to approach the quasistationary point $\hat{\mathbf{F}}$. For that matter, the iterates $F_\mu^{(n)}$ are expanded around the quasistationary point

$$F_\mu^{(n)}=\hat{F}_\mu+\delta_\mu^{(n)}.$$

Neglecting terms of order $(\delta_\mu^{(n)})^3$, the iteration (A1) can be rewritten as

$$\delta_\mu^{(n+1)}=\Delta\hat{C}_\mu+\hat{C}_{\mu\mu'}\delta_{\mu'}^{(n)}+\tfrac{1}{2}C_{\mu\mu'\mu''}\delta_{\mu'}^{(n)}\delta_{\mu''}^{(n)}, \qquad \text{(A4)}$$

where the quantities with a caret are taken at $(\{\hat{F}_{\mu''}\},\epsilon)$. The slowing down of the iteration is due to the component of δ_μ along the critical direction e^c. This component can be extracted by writing $\delta^{(n)}=a^{(n)}e^c$ and multiplying Eq. (A4) with the left eigenvector $\hat{e}^c$ of the stability matrix C. The resulting equation for $a^{(n)}$ is then

$$a^{(n+1)}-a^{(n)}=\sigma+(\lambda-1)(a^{(n)})^2. \qquad \text{(A5)}$$

Here we made use of Eq. (A2) and have normalized $e^c,\hat{e}^c$ such that $\Sigma_\mu\hat{e}_\mu^c e_\mu^c=1$. The quantities $\sigma=\Sigma_\mu\hat{e}_\mu^c\Delta C_\mu$ and λ

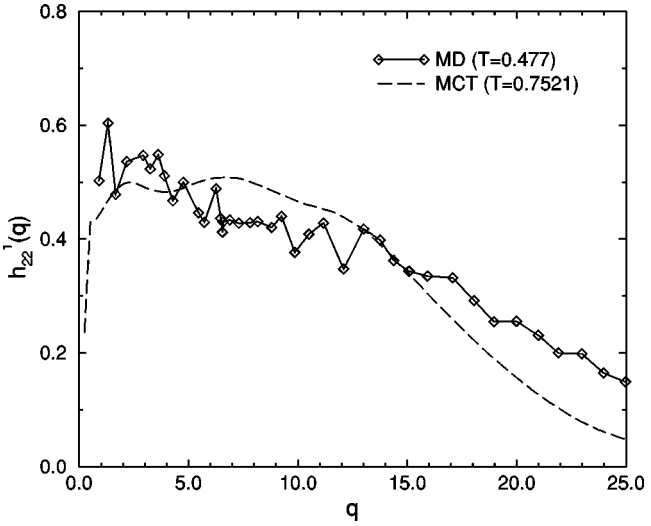

FIG. 7. Normalized critical amplitude $h_{22}^1(q)$. The critical amplitude of the simulation (full line) is multiplied with a free scale factor to optimize agreement with theory (see text for details). Shown is the theoretical result for $T=0.7521$ (dashed line).

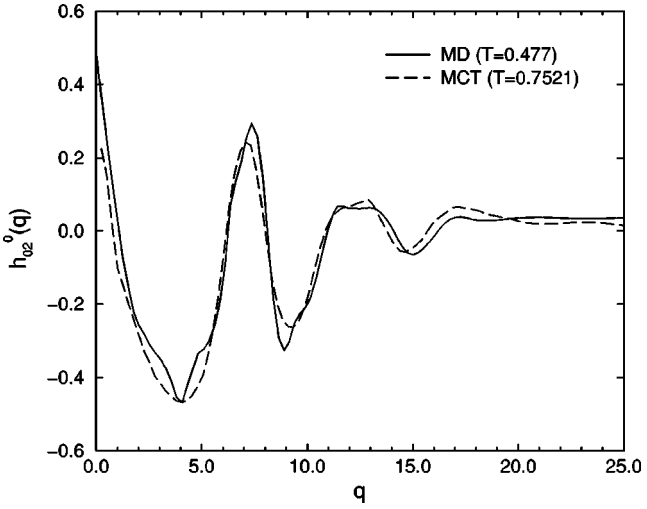

FIG. 8. Normalized critical amplitude $h_{02}^0(q)$. The critical amplitude of the simulation at $T=0.477$ (full line) is multiplied with a free scale factor to optimize agreement with theory (see text for details). Shown is the theoretical result for $T=0.7521$ (dashed line). Since the raw data of the simulations had to be smoothed, the data points are omitted.

$=1+\Sigma_\mu \hat{e}_\mu^c C_{\mu\mu'\mu''}\hat{e}_{\mu'}^c e_{\mu''}^c$ can be identified as the separation parameter and the exponent parameter $0<\lambda<1$ of the β-scaling theory, respectively [6,68]. Since consecutive iterates are very close to each other in the vicinity of $\hat{\mathbf{F}}$, we can rewrite Eq. (A5) as a differential equation,

$$-\dot{a}=[|\sigma|+(1-\lambda)a^2]. \tag{A6}$$

Let us assume we start the iteration at $t=0$ with $a(0)=a_0$. Then the solution of Eq. (A6) is

$$a(t)=-\frac{\sqrt{|\sigma|}}{\sqrt{1-\lambda}}\tan\left[\sqrt{(1-\lambda)|\sigma|}t-\arctan\left(a_0\frac{\sqrt{1-\lambda}}{\sqrt{|\sigma|}}\right)\right]. \tag{A7}$$

Since the iteration is initialized with a value for $\mathbf{F}$ slightly in the glass, the initial deviation a_0 from $\hat{\mathbf{F}}$ is of order $\sqrt{|\sigma|}=O(\sqrt{|\epsilon|})$. From Eq. (A7) it then follows that we need a number of iterations of the order $1/\sqrt{|\epsilon|}$ to approach $\hat{\mathbf{F}}$ [i.e., $a(t)=0$], and will stay close to $\hat{\mathbf{F}}$ [i.e., $a(t)\leqslant O(\sqrt{|\sigma|})$] for the same amount of iterations before the iterates decay to zero. This proves our statement that the quasistationary solution of the iteration for $T>T_c$ is approached with the same amount of iterations as the stable solution slightly below T_c. But there the glass solution agrees with $\mathbf{F}^c$ only up to order $\sqrt{\epsilon}$. The quasistationary solution $\hat{\mathbf{F}}$, however, agrees with $\mathbf{F}^c$ up to order $|\epsilon|\ll\sqrt{|\epsilon|}$.

[1] Here we always restrict ourselves to the idealized mode-coupling theory, which neglects all ergodicity restoring processes such as, e.g., hopping.

[2] W. van Megen and S. M. Underwood, Phys. Rev. Lett. **70**, 2776 (1993).

[3] W. van Megen and S. M. Underwood, Phys. Rev. E **49**, 4206 (1994).

[4] W. Kob and H. C. Andersen, Phys. Rev. E **51**, 4626 (1995); **52**, 4134 (1995).

[5] M. Nauroth and W. Kob, Phys. Rev. E **55**, 675 (1997).

[6] W. Götze, in *Liquids, Freezing and Glass Transition*, edited by J. P. Hansen, D. Levesque, and J. Zinn-Justin, Les Houches Session LI, 1989 (North-Holland, Amsterdam, 1991).

[7] W. Götze and L. Sjögren, Rep. Prog. Phys. **55**, 241 (1992).

[8] R. Schilling in *Disorder Effects on Relaxational Processes*, edited by R. Richert and A. Blumen (Springer, Berlin, 1994).

[9] Theme issue on *Relaxation Kinetics in Supercooled Liquids–Mode Coupling Theory and Its Experimental Tests*, edited by S. Yip [Transp. Theory Stat. Phys. **24**, (1995)].

[10] W. Götze, J. Phys.: Condens. Matter **11**, A1 (1999).

[11] H. Z. Cummins, J. Phys.: Condens. Matter **11**, A95 (1999).

[12] W. Kob, J. Phys.: Condens. Matter **11**, R85 (1999).

[13] F. Fujara and W. Petry, Europhys. Lett. **4**, 921 (1987).

[14] H. Z. Cummins, G. Li, W. Du, Y. H. Wang, and G. Q. Shen, Prog. Theor. Phys. Suppl. **126**, 21 (1997).

[15] L. J. Lewis and G. Wahnstrom, Phys. Rev. E **50**, 3865 (1994).

[16] S. Mossa, R. Di Leonardo, G. Ruocco, and M. Sampoli, e-print cond-mat/9912258.

[17] A. Tölle, J. Wuttke, H. Schober, O. G. Randl, and F. Fujara, Eur. Phys. J. B **5**, 231 (1998).

[18] W. Knaak, F. Mezei, and B. Farago, Europhys. Lett. **7**, 529 (1991).

[19] G. Li, W. M. Du, X. K. Chen, and H. Z. Cummins, Phys. Rev. A **45**, 3867 (1992); H. Z. Cummins *et al.*, Phys. Rev. E **47**, 4223 (1993); N. J. Tao *et al.*, Phys. Rev. A **44**, 6665 (1991).

[20] Y. Yang and K. A. Nelson, in Disordered Materials and Interfaces, edited by H. Z. Cummins, D. J. Durian, D. L. Johnson, and H. E. Stanley, Mater. Res. Soc. Symp. Proc. No. 407 (Materials Research Society, Pittsburgh, 1996), p. 147.

[21] P. Lunkenheimer, A. Pimenov, M. Dressel, B. Schreier, U.

Schneider, and A. Loidl, Prog. Theor. Phys. Suppl. **126**, 123 (1997).
[22] J. Wuttke, J. Hernandez, G. Li, G. Coddens, H. Z. Cummins, F. Fujara, W. Petry, and H. Sillescu, Phys. Rev. Lett. **72**, 3052 (1994).
[23] J. Wuttke, W. Petry, G. Coddens, and F. Fujara, Phys. Rev. E **52**, 4026 (1995).
[24] P. Lunkenheimer, A. Pimenov, M. Dressel, Y. G. Goncharov, R. Böhmer, and A. Loidl, Phys. Rev. Lett. **77**, 318 (1996).
[25] G. Li, W. M. Du, A. Sakai, and H. Z. Cummins, Phys. Rev. A **46**, 3343 (1992).
[26] Y. Yang and K. A. Nelson, Phys. Rev. Lett. **74**, 4883 (1995).
[27] Y. Yang and K. A. Nelson, J. Chem. Phys. **103**, 7732 (1995).
[28] J. Wuttke, M. Seidl, G. Hinze, A. Tölle, W. Petry, and G. Coddens, Eur. Phys. J. B **1**, 169 (1998).
[29] F. Sciortino, P. Gallo, P. Tartaglia, and S.-H. Chen, Phys. Rev. E **54**, 6331 (1996); P. Gallo, F. Sciortino, P. Tartaglia, and S.-H. Chen, Phys. Rev. Lett. **76**, 2730 (1996).
[30] F. Sciortino, L. Fabbian, S. H. Chen, and P. Tartaglia, Phys. Rev. E **56**, 5397 (1997).
[31] C. Theis and R. Schilling, Phys. Rev. E **60**, 740 (1999).
[32] T. Franosch, M. Fuchs, W. Götze, M. R. Mayr, and A. P. Singh, Phys. Rev. E **56**, 5659 (1997).
[33] H. Z. Cummins, G. Li, W. Du, R. M. Pick, and C. Dreyfus, Phys. Rev. E **53**, 896 (1996); **55**, 1232 (1997).
[34] R. Torre, P. Bartolini, and R. Pick, Phys. Rev. E **57**, 1912 (1998).
[35] G. Hinze, D. S. Brace, S. D. Gottke, and M. D. Fayer, Phys. Rev. Lett. **11**, 2437 (2000).
[36] H. Sillescu and E. Bartsch, in *Disorder Effects on Relaxational Processes*, edtied by R. Richert and A. Blumen (Springer, Berlin, 1994).
[37] E. Rössler and M. Taupitz, in *Disorder Effects on Relaxational Processes*, edited by R. Richert and A. Blumen (Springer, Berlin, 1994).
[38] H. W. Spiess and K. Schmidt-Rohr, in *Disorder Effects on Relaxational Processes*, edited by R. Richert and A. Blumen (Springer, Berlin, 1994).
[39] L. Andreozzi, A. Di Schino, M. Giordano, and D. Leporini, Europhys. Lett. **38**, 669 (1997).
[40] U. Bengtzelius, W. Götze, and A. Sjölander, J. Phys. C **17**, 5915 (1984).
[41] C. Bennemann, W. Paul, K. Binder, and B. Dünweg, Phys. Rev. E **57**, 843 (1998).
[42] W. Götze and M. Mayr, Phys. Rev. E **61**, 587 (2000).
[43] W. Götze, A. P. Singh, and Th. Voigtmann, Phys. Rev. E **61**, 6934 (2000).
[44] S. H. Chong and F. Hirata, Phys. Rev. E **58**, 6188 (1998).
[45] This notation is used to distinguish the molecular approach from the site-site description.
[46] R. Schilling and T. Scheidsteger, Phys. Rev. E **56**, 2932 (1997); T. Scheidsteger and R. Schilling, Philos. Mag. B **77**, 305 (1998).
[47] L. Fabbian, A. Latz, R. Schilling, F. Sciortino, P. Tartaglia, and C. Theis, Phys. Rev. E **60**, 5768 (1999).
[48] K. Kawasaki, Physica A **243**, 25 (1997).
[49] A. Latz, J. Non-Cryst. Solids **235-237**, 128 (1998).
[50] M. Letz, R. Schilling, and A. Latz, e-print cond-mat/9906336.
[51] L. Fabbian, A. Latz, R. Schilling, F. Sciortino, P. Tartaglia, and C. Theis, Phys. Rev. E (to be published); e-print cond-mat/9812363, 1998 (unpublished).
[52] C. Theis, F. Sciortino, A. Latz, R. Schilling, and P. Tartaglia, Phys. Rev. E (to be published); e-print cond-mat/0003508.
[53] J. Ram and Y. Singh, Phys. Rev. A **44**, 3718 (1991).
[54] J. Ram, R. C. Singh, and Y. Singh, Phys. Rev. E **49**, 5117 (1994).
[55] M. Letz and A. Latz, Phys. Rev. E **60**, 5865 (1999).
[56] S. Kämmerer, W. Kob, and R. Schilling, Phys. Rev. E **58**, 2131 (1998).
[57] S. Kämmerer, W. Kob, and R. Schilling, Phys. Rev. E **58**, 2141 (1998).
[58] C. Theis and R. Schilling, J. Non-Cryst. Solids **235-237**, 106 (1998).
[59] C. G. Gray and K. E. Gubbins, *Theory of Molecular Fluids* (Clarendon Press, Oxford, 1984), Vol. 1.
[60] C. Theis (private communication).
[61] Note that our definition of the stability matrix differs by a similarity transformation $\mathbf{A}\hat{\mathbf{C}}\mathbf{A}^{-1}$ from the one in [6].
[62] W. Götze, Z. Phys. B: Condens. Matter **56**, 139 (1984).
[63] W. Götze, Z. Phys. B: Condens. Matter **60**, 195 (1985).
[64] T. Franosch, M. Fuchs, W. Götze, M. R. Mayr, and A. P. Singh, Phys. Rev. E **55**, 7153 (1997).
[65] J.-L. Barrat, W. Götze, and A. Latz, J. Phys.: Condens. Matter **1**, 7163 (1989).
[66] W. van Megen and S. M. Underwood, Phys. Rev. E **47**, 248 (1993).
[67] J.-L. Barrat and A. Latz, J. Phys.: Condens. Matter **2**, 4289 (1990).
[68] Note that our definition of $C_{\mu\mu'\mu''}$ differs from the one used in [6] analogous to [61].